Available online at www.sciencedirect.com
ScienceDirect
Trans. Nonferrous Met. Soc. China 24(2014) 1653−1658
Transactions of Nonferrous Metals Society of China
www.tnmsc.cn

Influence of Li addition on mechanical property and aging precipitation behavior of Al−3.5Cu−1.5Mg alloy

Yun-lai DENG, Jin-long YANG, Si-yu LI, Jin ZHANG, Xin-ming ZHANG

School of Materials Science and Engineering, Central South University, Changsha 410083, China

Received 22 May 2013; accepted 18 March 2014

Abstract: The influence of Li addition on mechanical property and aging precipitation behavior of Al−3.5Cu−1.5Mg alloy was investigated by tensile test, scanning electron microscopy (SEM), transmission electron microscopy (TEM) and high resolution transmission electron microscopy (HRTEM). The results show that the tensile strength can be significantly improved with the slightly decreased ductility and the form of fracture morphology is converted from ductile fracture into ductile/brittle mixed fracture by adding 1.0% Li. Besides, the peak aging time at 185 °C is delayed from 12 to 24 h and the main precipitation phase $S'(Al_2CuMg)$ is converted into S' $(Al_2CuMg)+\delta'(Al_3Li)$, while the formation of $S'(Al_2CuMg)$ is delayed.

Key words: aluminum alloy; Al−3.5Cu−1.5Mg alloy; Li; aging behavior; mechanical properties

1 Introduction

Al−Cu−Mg alloys generally have a desirable combination of density, strength, damage tolerance, which are suitable for aeronautical and aerospace components [1]. The strengthening effect of the Al−Cu−Mg alloys leans mainly upon the volume fraction and radius of the second phase [2,3]. For Al−Cu−Mg alloys in the α+S phase field, the precipitation sequence is as follows [4,5]:

$$SSS \rightarrow GPB/co\text{-}clusters \rightarrow GPB2/S'' \rightarrow S'/S\ (Al_2CuMg)$$

where SSS stands for supersaturated solid solution. The S'' can be understood as a phase which is highly coherent with Al matrix. The S phase, which forms as laths on $\{210\}_{Al}$ habit planes, is elongated along $\langle 100\rangle_{Al}$. Orthorhombic crystal structure (*Cmcm*, a=0.400 nm, b=0.923 nm, c=0.714 nm) is the stable structure of S phase [4,5].

Micro-alloying additions are known to affect precipitation processes of Al−Cu−Mg alloys in many ways, so that the response to age-hardening is enhanced [4−6]. A group of potentially age-hardenable alloys, which are around the composition range Al−(2−4)Cu−(1−2)Mg with Mn [6], Sn [7], Ag [8], Zr and/or Sc [6] additions , have been investigated.

Lithium is the lightest metallic element, which reduces the density and increases the modulus of Al-based alloys. The presence of Li in Al−Cu−Mg alloy can cause a range of new phases. Aging precipitations in Al−Cu−Mg−Li alloy are as follows: $S(Al_2CuMg)$; $\theta'(Al_2Cu)$; $T_1(Al_2CuLi)$; $\delta'(Al_3Li)$[4,9−11]. In high-copper alloys, such as AA 2050 (Al−3.5Cu−1.3Li−0.6Mg [9]), the plate-shaped T_1 (Al_2CuLi) phase nucleating on {111} matrix plane plays an important role in precipitation strengthening. And $\theta'(Al_2Cu)$, $T_1(Al_2CuLi)$ phases can be observed in AA 2195 Al−4.01Cu−1.1Li−0.39Mg−0.19Zr alloy [10]. In Al−Cu−Mg−Li(Mn,Zr) alloy, another precipitation sequence has been reported, which is different from the sequence in α+S phase field Al−Cu−Mg alloys [11].

$$SSS \rightarrow \delta'(Al_3Li) \rightarrow \delta(AlLi)$$

where δ' is an $L1_2$ ordered phase (Al_3Li) and fully coherent with the Al matrix, and δ is equilibrium Al−Li phase.

However, it is not available that the systematical study about the effect of Li addition on microstructure and properties of Al−3.5Cu−1.5Mg alloy. In Al−3.5Cu−1.5Mg alloy, mole ratio of copper to magnesium is about 1. The purpose of this work is to study the effect of Li addition on microstructures and properties of Al−3.5Cu−1.5Mg alloy (in α+S phase field), to highlight

Foundation item: Projects (2010CB731700, 2012CB619500) supported by the National Basic Research Program of China
Corresponding author: Yun-lai DENG; Tel: +86-731-88876931; E-mail: luckdeng@csu.edu.cn
DOI: 10.1016/S1003-6326(14)63237-4

how the Li addition alters the main properties and precipitation, and to explore the interaction between *S* (Al_2CuMg) and δ'(Al_3Li).

2 Experimental

Two kinds of investigated alloys were prepared through ingot metallurgical route in the laboratory and cast in argon atmosphere. Raw materials included high purity Al (99.998%), Mg (purity 99.98%), Zn (purity 99.98%), Al−30%Cu, Al−15%Mn, Al−3%Li, Al−5%Ti−B. The alloys were melted in a graphite crucible and heated by an electrical resistance furnace. The temperatures of melting, refining and casting were 750−780 °C, 730−750 °C, 720−730 °C, respectively. Liquid metal was then poured into an iron mold to obtain 30 mm×80 mm×120 mm (thickness × width × length) ingot. The chemical composition of the alloys is shown in Table 1. After being homogenized at 490 °C for 24 h, the ingots would be hot-rolled and cold-rolled to 3 mm-thick sheets at the initial rolling temperature of 420 °C. Samples cut from the sheets were solution treated at 510 °C for 2 h, followed by being quenched into water at room temperature and subsequently aging at 185 °C for various time.

In order to study the effects of Li addition in Al−Cu−Mg alloy, tensile specimens were sectioned parallel to the rolled direction. AJSM−6360LV scanning electron microscope (SEM) and TECNAIG^{2}20 transmission electron microscope at an acceleration voltage of 200 kV were used to study the second phase. Specimens for transmission electron microscopy (TEM) and high resolution transmission electron microscopy (HRTEM) were prepared by mechanical grinding and twin-jet electropolishing.

Table 1 Chemical composition of studied aluminum alloys (mass fraction, %)

Alloy No.	Cu	Mg	Mn	Ti	Zn	Li	Al
1	3.47	1.45	0.46	0.06	0.21	−	Bal.
2	3.46	1.46	0.49	0.07	0.19	1.01	Bal.

3 Results and analysis

3.1 Mechanical property

The tensile test results of the two Al alloys are shown in Fig. 1. The results show that, with the increase of aging time, the strengths of the two alloys increase to their peak and then decrease while the ductilities decrease a little. And obviously, the aging precipitation behavior of the Al−3.5Cu−1.5Mg alloy can be affected by the addition of Li. The peak aging strength is improved by 20 MPa and the ductility decreases from 20.1% to 15.8%. Meanwhile, the time of the peak aging is delayed significantly.

SEM fractographs of the two specimens under 185 °C peak aging conditions are shown in Fig. 2. It can be observed that these fracture surfaces are mainly composed of ductile transgranular fracture and ductile intergranular fracture. For the two alloys, owing to the addition of Li, the dominating fracture type changes from dimple fracture to intergranular fracture. This is consistent with the decrease of the elongation, as shown in Fig. 1.

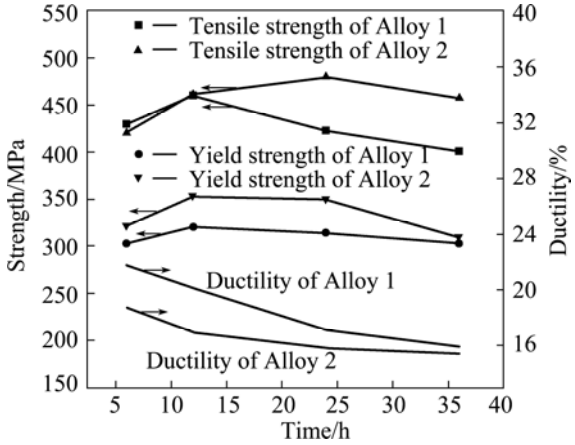

Fig. 1 Mechanical properties of two alloys

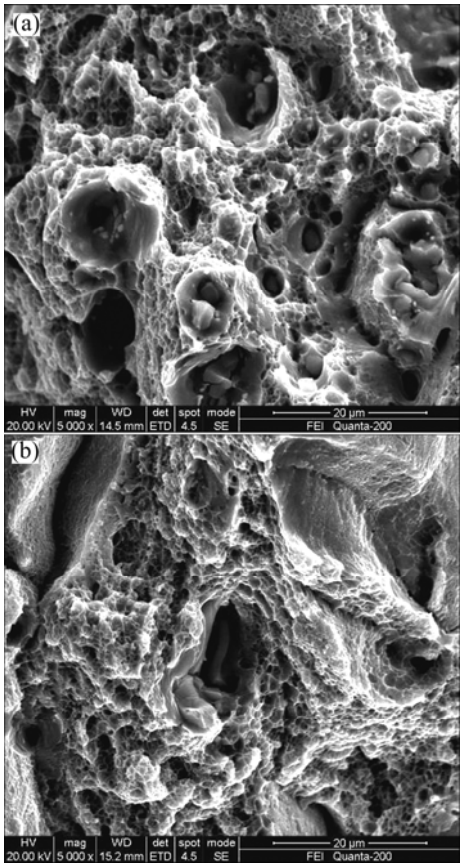

Fig. 2 SEM fractographs of two specimens peak aged at 185 °C: (a) Alloy 1; (b) Alloy 2

3.2 Aging precipitation behavior

TEM and HRTEM images of Alloy 1 aged at 185 °C for 12 h are shown in Fig. 3. TEM bright field micrograph and selected area electron diffraction (SAED) (beam direction [100]) are shown in Figs. 3(a) and (b) respectively. Figure 3(a) indicates the presence of at least two phases in the Al matrix. The larger dispersed phase is known to be *T* phase ($Al_{20}Cu_2Mn_3$),which is Mn-rich phase and commonly found in aluminum alloys containing Mg, Cu, Mn [4,11,12]. Except for *S*′, no streaking or other diffraction effects appear on the selected area diffraction patterns.

With regard to *S*′ phase, Fig. 3(c) shows the HRTEM image of *S*′ phase, and the fast Fourier transform (FFT) of the corresponding region is shown in Fig. 3(d). This pattern has already been identified in Refs. [4,13] as the variant of *S*′ phase.

A typical bright field TEM image obtained for Alloy 2 aged at 185 °C for 12 h is shown in Fig. 4. As shown in Fig. 4(a), the co-existence of *S*′ phase and *δ*′ phase (Al_3Li) is observed. The *S*′ precipitates are arranged in groups of ring-shaped agglomerates. The similar phenomenon has been reported in Refs. [4,13]. The existence of *δ*′ phase has been identified in Fig. 4(b). The *δ*′ phase, whose lattice constant equals 0.4308 nm [4], is only slightly smaller than that of the Al matrix, so that the coffee bean-like phase precipitates coherently in a spherical shape. The spots due to the *δ*′(Al_3Li) phase are observed at $(1/2)111_{Al}$ and its equivalent positions [14]. In Fig. 4(c), several typical phase morphologies can be observed, such as *T* ($Al_{20}Cu_2Mn_3$) phase, *δ*′ (Al_3Li) phase, *S*′ phase and *S*″ phase. The volume fraction of the needle-like *S*′ precipitates is obviously less than Alloy 1, as shown in Fig. 3(a). Besides, it can be observed that some black spots exist in Fig. 4(c), and the corresponding HRTEM and FFT images are shown in Fig. 4(d). It can be inferred that the black spots are *S*″ phase. The similar phenomenon has been reported in many relative literatures [2,4,13,15−17]. This means that the *S*″ phase and *S*′ phase coexist in Alloy 2 under this aging condition. While in Alloy 1, which contains no lithium, only *S*′ phase was found. Thus the addition of Li slows down the *S*′ phase formation rate. Due to the fact that the binding energy of Li with vacancy is similar to Mg (Mg 0.19 eV, Li 0.26 eV) [10], the mobility of vacancies is reduced by the formation of Li-vacancy pairs, and then the formation of Cu−Mg clusters is delayed.

After aging at 185 °C for 24 h, the bright field (BF) and SAED images of the two alloy specimens are shown in Fig. 5. The *S*′ phase and the *δ*′ phase can be obviously observed in Figs. 5(a) and (b) respectively. The SAED

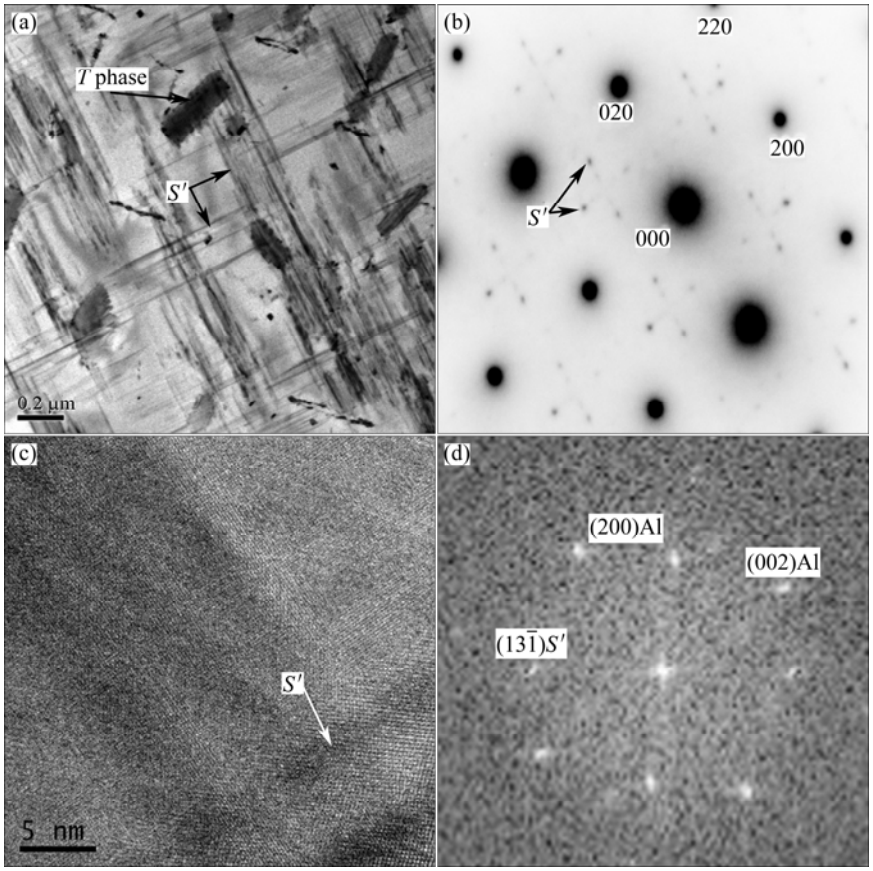

Fig. 3 TEM image (a) and SAED pattern (b) of Alloy 1 aged at 185 °C for 12 h (beam direction [100]), HRTEM image (c) of *S*′ phase and FFT (d) of corresponding region in (c)

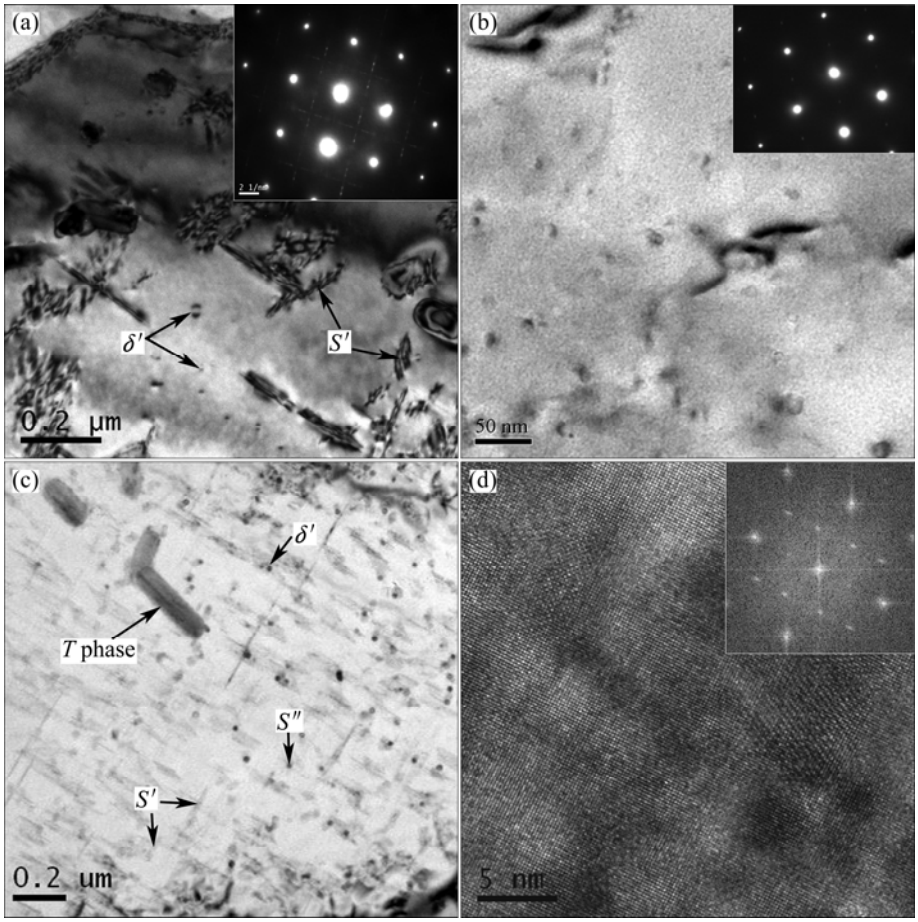

Fig. 4 TEM, SAED and HRTEM micrographs of Alloy 2 aged at 185 °C for 12 h: (a) Intrageranular precipitates in ⟨100⟩ direction; (b) Intrageranular precipitates in ⟨110⟩ direction; (c) Intrageranular precipitates in ⟨100⟩ direction, in which *S*″ phase can be seen; (d) HRTEM and FFT patterns in ⟨100⟩ direction

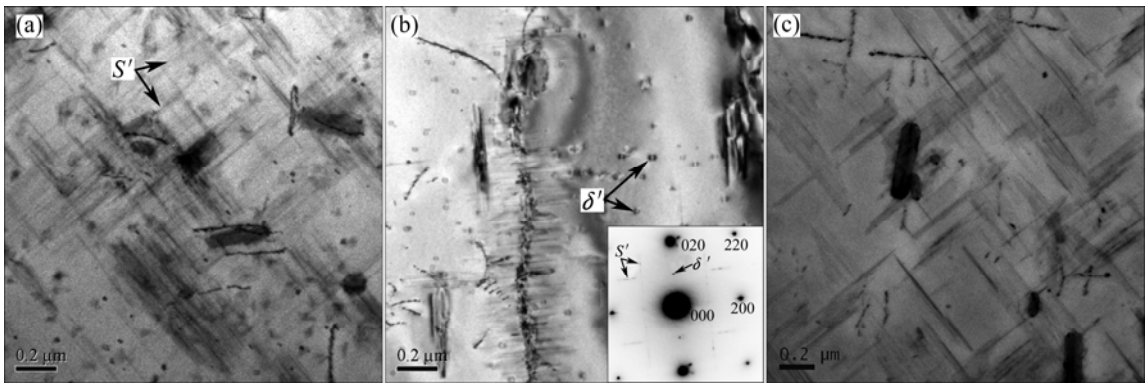

Fig. 5 TEM and SAED patterns in ⟨100⟩ direction of Alloy 2 (a, b) and Alloy 1 (c) aged at 185 °C for 24 h

pattern in Fig. 5(b) shows super lattice spots from the *δ*′ (Al_3Li) phase ($(1/2)002_{Al}$ and its equivalent positions) and spots from the *S*′ phase.

The co-existence of *S*′ phase and *δ*′ phase in Alloy 2, which is different from the single existence of the *S*′ phase in Alloy 1, is clear due to the addition of 1.0% Li. And this change in the microstructure can be considered the cause of property difference between the two alloys. It is worth noting that in previous literatures, the notable effect of *δ*′ (Al_3Li) phase on aging strengthening has been only found in Al−Cu−Mg−Li alloys with high Li content (1.4%−1.5%), such as 2091 Al alloy [12,18].

Figure 6 shows the TEM images near the grain boundary of the two alloys at peak aging condition. It can be observed that the precipitate-free zone (PFZ) in Alloy 1 appears wider than that in Alloy 2, the width of the PFZ is about 70 nm in Alloy 1 and 30 nm in Alloy 2. PFZ is caused by deleted solution atoms around the grain

boundary [19,20]. As mentioned earlier, the existence of Li atoms reduces the number of mobile vacancies, which makes the formation of grain boundary precipitation (GBP) difficult. These cause the surrounding solution atoms consumption decrease. More solution atoms form Cu−Mg atom clusters, which will develop to *S*′ around grain boundary, thus PFZ appears narrow in Alloy 2.

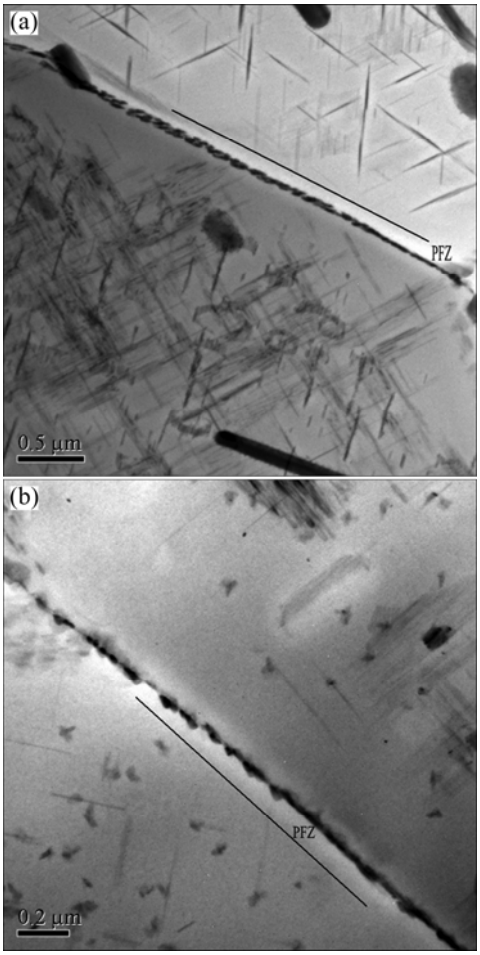

Fig. 6 PFZ of two alloys aged under 185 °C peak aging condition: (a) Alloy 1 aged at 185 °C for 12 h; (b) Alloy 2 aged at 185 °C for 24 h

It has been clearly attested that the ductility of Li-containing 2xxx aluminum alloys is closely related to the PFZ [12]. Strain localization that results from the planar slip of shearable precipitates, such as δ' phase, also plays a crucial role in the Al−Li alloys [21]. Once deformation has occurred on a particular glide plane, especially around the δ' phase, the dislocation movement by slip will occur on the same plane. Then the dislocations can be accumulated around the grain boundary, and this always causes the stress concentration [20]. Hence, cracks can nucleate and result in failure of the material. This can also be supported by the SEM images, as shown in Fig. 2, in which ductile/brittle mixed fracture is obvious. Based on the discussion above, it can be accepted that the ductility of Alloy 2 is lower.

4 Conclusions

1) The peak aging time of Al−3.5Cu−1.5Mg alloy can be delayed significantly by the addition of 1.0% Li. The peak aging strength is improved by 20 MPa, while the ductility decreases from 20.1% to 15.8%.

2) The addition of lithium (1.0%) can change the precipitation of the Al−3.5Cu−1.5Mg alloy from *S*′ (Al_2CuMg) phase to *S*′ (Al_2CuMg) and δ' (Al_3Li) phases.

3) Lithium postpones the formation of *S*′ (Al_2CuMg) phase in Al−3.5Cu−1.5Mg alloy and makes PFZ narrow.

References

[1] STARKE E A, STALELY J T. Application of modern aluminum alloys to aircraft [J]. Prog Aerospace Science, 1996, 32: 131−172.

[2] WANG S C, STARINK M J, GAO N. Precipitation hardening in Al−Cu−Mg alloys revisited [J]. Scripta Materialia, 2006, 54(2): 287−291.

[3] RALSTON K D, BIRBILIS N, WEYLAND M, HUTCHINSON C R. The effect of precipitate size on the yield strength-pitting corrosion correlation in Al−Cu−Mg alloys [J]. Acta Materialia, 2010, 58(18): 5941−5948.

[4] WANG S C, STARINK M J. Precipitates and intermetallic phases in precipitation hardening Al−Cu−Mg−(Li) based alloys [J]. International Materialia Review, 2005, 50(4): 193−215.

[5] SHA G, MARCEAU R K W, GAO X. Nanostructure of aluminium alloy 2024: Segregation, clustering and precipitation processes [J]. Acta Materialia, 2011, 59(4): 1659−1670.

[6] STARINK M J, GAO N, KAMP N, WANG S C. Relations between microstructure, precipitation, age-formability and damage tolerance of Al−Cu−Mg−Li (Mn, Zr, Sc) alloys for age forming [J]. Materials Science and Engineering A, 2006, 418(1−2): 241−249.

[7] SANJIB B, ROBI P S. Effect of trace additions of Sn on microstructure and mechanical properties of Al−Cu−Mg alloys [J]. Materials Design, 2010, 31(8): 4007−4015.

[8] BANKAVORS D, PANKGNELL P B, BES B. The effect of silver on microstructural evolution in two 2xxx series Al-alloys with a high Cu:Mg ratio during ageing to a T8 temper [J]. Materials Science and Engineering A, 2008, 491(1−2): 214−223.

[9] LEQUEN P H, SMITH K P, DANIELOU A. Aluminum−copper−lithium alloy 2050 developed for medium to thick plate [J]. Journal of Materials Engineering and Performance, 2010, 19(6): 841−847.

[10] HUANG Bi-ping, ZHENG Zi-qiao. Independent and combine roles of trace Mg and Ag addition in properties precipitation process and precipitation kinetics of Al−Cu−Li−(Mg)−(Ag)−Zr−Ti [J]. Acta Metallurgica, 1998, 46(12): 4381−4393.

[11] DENG Yun-lai, ZHOU Liang, JIN Kun, ZHANG Xin-ming. Microstructure and properties of creep aged 2124 aluminum alloy [J]. Transactions of Nonferrous Metals Society of China, 2010, 20(11): 2106−2111.

[12] ZHANG Jin, DENG Yun-lai, LI Si-yu, CHEN Ze-yu. Creep age forming of 2124 aluminum alloy with single/double curvature [J]. Transactions of Nonferrous Metals Society of China, 2013, 23(7): 1922−1929.

[13] ENRIQUE J L, NICHOLAS J G. Review aluminium−lithium alloys [J]. Journal of Materials Science, 1987, 22(5): 1521−1529.

[14] NOVELO O P, FIHUEROA I A, LARA G R. New evidence on the nature of the metastable *S*″-phase on Al−Cu−Mg alloys [J]. Materials Chemistry and Physics, 2011, 130(1−2): 431−436.

[15] LI Hong-ying, TANG Yi, ZENG Zai-de. Effect of ageing time on strength and microstructures of an Al−Cu−Li−Zn−Mg−Mn−Zr alloy [J]. Materials Science and Engineering A, 2008, 498(1−2): 314−320.
[16] WANG S C, STARINK M J. The assessment of GP*B*2/*S*″ structures in Al−Cu−Mg alloys [J]. Materials Science and Engineering A, 2004, 386(1−2):156−163.
[17] KOVARIK L, COYRT S A,FRASER H L, MILLS M J. GPB zones and composite GPB/GPBII zones in Al−Cu−Mg alloys [J]. Acta Materialia, 2008, 56(17): 4804−4815.
[18] STARINK M J, WANG P, SINCLAIR I, GREGSON P J. Microstrucure and strengthening of Al−Li−Cu−Mg alloys and MMCS:I Analysis and modeling of microstructural changes [J]. Acta Materialia, 1999, 47(14): 3841−3851.
[19] GANDIN C A, JACOT A. Modeling of precipitate-free zone formed upon homogenization in a multi-component alloy [J]. Acta Materialia, 2007, 55(7): 2539−2553.
[20] STARINK M J. Reduced fracturing of intermetallic particles during crack propagation in age hardening Al-based alloys due to PFZs [J]. Materials Scinece and Engineering A, 2005, 390(1−2): 260−264.
[21] ZHU A W, STRAKE E A. Strengthening effect of unshearable particles of finite size: A computer experimental study [J]. Acta Materialia, 1999, 47(11): 3263−3269.

Li 对 Al−3.5Cu−1.5Mg 合金力学性能与时效析出行为的影响

邓运来，杨金龙，李思宇，张 劲，张新明

中南大学 材料科学与工程学院，长沙 410083

摘 要：采用拉伸实验、扫描电子显微分析(SEM)、透射电子显微分析(TEM)、高分辨电子显微技术研究 Li 添加对 Al−3.5Cu−1.5Mg 合金力学性能与时效析出行为的影响。结果表明：添加 1.0%Li 能使 Al−3.5Cu−1.5Mg 合金的峰值时效拉伸强度明显提高，伸长率略有下降。峰值时效拉伸样品的断口形貌由韧断口转变为韧/脆混合型。Li 使合金 185 °C 峰值时效时间由 12 h 延长至 24 h，析出相由 *S*′(Al_2CuMg) 转变为 *S*′(Al_2CuMg)+*δ*′(Al_3Li)。在 Al−3.5Cu−1.5Mg−1.0Li 合金中，*S*′(Al_2CuMg)相时效析出延缓。

关键词：铝合金；Al−3.5Cu−1.5Mg 合金；Li；时效行为；力学性能

(Edited by Xiang-qun LI)